

# Autoencoders with Intrinsic Dimension Constraints for Learning Low Dimensional Image Representations

Jianzhang Zheng, Hao Shen, Jian Yang, Xuan Tang,  
Mingsong Chen, Hui Yu, Jielong Guo, Xian Wei\*

**Abstract**—Autoencoders have achieved great success in various computer vision applications. The autoencoder learns appropriate low dimensional image representations through the self-supervised paradigm, i.e., reconstruction. Existing studies mainly focus on the minimizing the reconstruction error on pixel level of image, while ignoring the preservation of Intrinsic Dimension (ID), which is a fundamental geometric property of data representations in Deep Neural Networks (DNNs). The learning process of DNNs is observed involving highly with the change of the ID of data representations. Motivated by the important role of ID, in this paper, we propose a novel deep representation learning approach with autoencoder, which incorporates regularization of the global and local ID constraints into the reconstruction of data representations. This approach not only preserves the global manifold structure of the whole dataset, but also maintains the local manifold structure of the feature maps of each point, which makes the learned low-dimensional features more discriminant and improves the performance of the downstream algorithms. To our best knowledge, existing works are rare and limited on exploiting both global and local ID invariant properties on the regularization of autoencoders. Numerical experimental results on benchmark datasets (Extended Yale B, Caltech101 and ImageNet) show that the resulting regularized learning models achieve better discriminative representations for downstream tasks including image classification and clustering.

## I. INTRODUCTION

Recently, Deep Neural Networks (DNNs) have been successfully applied to various high-dimensional machine learning tasks, such as computer vision and natural language processing [12], [9], [28]. Instead of learning the mapping relationship, DNNs learn the intrinsic geometric structure of data representations and flatten the data in higher layers [1], [6]. The learning process of data representations in DNNs often involves layer-wise changes in features for their inputs, e.g., dimension increase and dimension reduction.

Intrinsic Dimension (ID) is a fundamental geometrical property of data representations in DNNs, which is the minimum number of variables or parameters needed to describe points in the ambient space with little information loss [34], [15], [1], [2]. Correspondingly, the dimension of ambient space is

referred to as Extrinsic Dimension (ED). Although the ED of data representations is high, data are often concentrated around a low-dimensional manifold [42], [40], [4], and the ID of the high-dimensional data representations can be defined as the dimension of the embedded manifold [1], [2]. The ID can also be defined by comparing with a series of distributions with known dimension, and the dimension of the distribution with the most similar characteristics is the desired ID [15], [2].

As revealed in the research field of self-supervised representation learning [13], [38], [20], [25], [3], the intrinsic structure information of observed data learned by self-supervised models have the capability of discrimination that is useful for downstream tasks. AutoEncoder (AE) is a classical and effective self-supervised representation learning paradigm through encoding and decoding maps to get compact and discriminative low-dimensional representations [4]. In recent years, amounts of AE-based models have been proposed and they develop strategies to employ the spatial, temporal, spectral and context structure information of inputs [45], [31], [25]. Inspired by the powerful representation capability and success of these strategies, this work explores how the ID can be used to preserve the intrinsic manifold structure of representations improve the performance on the downstream tasks. To our best of knowledge, it is still an important pending question of how to develop AE that exploit both global and local ID knowledge.

In this paper, we attempt to answer this question by exploiting the ID information in data representations to preserve the global and local manifold structure during transformation. Our generic approach can be applied in various forms of AE, but the training paradigm is different from the vanilla AE, which considers global and local ID loss during reconstruction, shown in Fig. 1. The main contributions of this paper are summarized as follows:

- The proposed method exploits ID information of data representations from global and local perspectives, i.e., the global ID for whole sample data points and the local ID for feature maps from each point.
- A generic ID-based regularization is incorporated into the current standard autoencoder framework to develop a new training paradigm, coined as AutoEncoder with Intrinsic Dimension Constraint (AE-IDC), which manages to maintain ID invariant along with reconstruction.
- The AE-IDC achieves more discriminative compressed representations than existing AE models based on Convolutional Neural Networks (CNNs) and Vision Transform-

\* Corresponding Author

Jianzhang Zheng is with the Technical University of Munich, and also with the Fujian Institute of Research on the Structure of Matter, Chinese Academy of Science (e-mail: zhengjianzhang@fjirsm.ac.cn). Hao Shen is with the fortiss GmbH (e-mail: shen@fortiss.org). Jian Yang is with the Information Engineering University (e-mail: jian.yang@tum.de). Xuan Tang and Mingsong Chen are with the East China Normal University (e-mail: xtang@cee.ecnu.edu.cn; mschen@sei.ecnu.edu.cn). Hui Yu and Jielong Guo are with the Fujian Institute of Research on the Structure of Matter, Chinese Academy of Science (e-mail: yuhui@fjirsm.ac.cn; gjl@fjirsm.ac.cn). Xian Wei is with the Technical University of Munich (e-mail: xian.wei@tum.de).

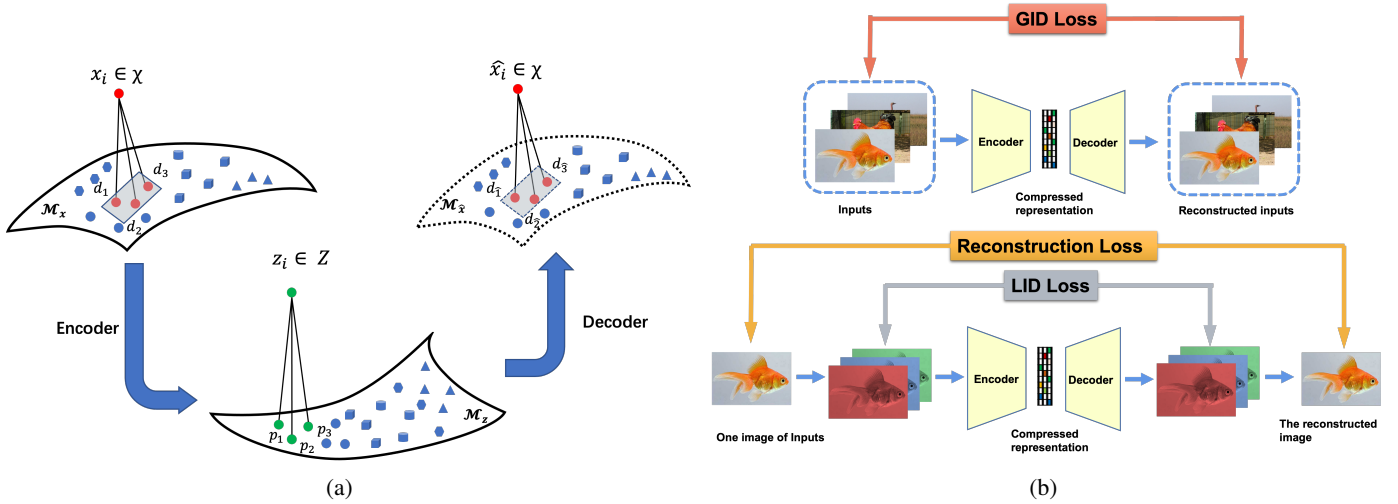


Fig. 1: Overview of training paradigm of AE-IDC. GID: global intrinsic dimension; LID: local intrinsic dimension. (a) The goal of AE-IDC is to get compressed representations while maintaining data manifold structure globally and locally during the process of encoding and decoding. (b) An illustration of reconstruction loss, GID loss and LID loss on an image dataset.

ers (ViT) on small scale, middle-level scale and large scale datasets: Extended Yale B [19], Caltech101 [17], and ImageNet [41].

## II. RELATED WORK

### A. Self-supervised Representation Learning

Autoencoding is a classical paradigm in self-supervised learning, which is widely used in dimensional reduction, denoising and generation. It consists of two parts: the encoder maps the input to latent space, and the decoder reconstructs the input. There are various self-supervised learners based on autoencoding, such as Principal Component Analysis (PCA) [22], Denoising AE (DAE) [43], Variational AE (VAE) [32], Generative Adversarial Networks (GAN) [23]. Leveraging modern architectures in DNNs such as Residual Networks (ResNet) [27] and ViT [14], it can deal with large-scale data efficiently. Recently, Masked AutoEncoders (MAE) [25] and its convolutional variant [18], driven by the reconstruction from partially random masked samples, achieve state-of-the-art performances in downstream vision tasks. The proposed training framework can enhance MAE’s learning through imposing ID constraints.

Besides AE-based learners, contrastive learning is another popular paradigm in self-supervised learning. The contrastive learning methods such as MoCo [26], SimCLR [10] and DINO [7] do not require the model to be able to reconstruct the original input, but instead expects the model to learn discriminative representations in the embedding space by maximizing the distance between different points and minimizing the distance between different augmented representations from the same data point.

### B. Intrinsic Dimension Estimation Techniques

The concept of Intrinsic Dimension (ID) has gained significant attention because it helps in learning the underlying

manifold of high-dimensional data. ID is a powerful tool that quantitatively measures the intrinsic geometric structure of data representations. It also serves as a lower bound of the dimension reduction of the dataset and a measurement of the complexity of the dataset. Accurate ID can help to understand the structure of data representations, and guide the design of DNNs in terms of their width and depth. The overestimation of ID brings additional computational overhead, whereas the underestimation of ID results in significant information loss.

A number of estimation methods have been developed, and they are generally grouped into global or local class [2]. Global methods consider the entire dataset to provide a single Global Intrinsic Dimension (GID) estimation for the dataset. Some of the typical algorithms include correlation dimension [24], DANCo [8] and TwoNN [15]. Local methods analyze each data point’s neighborhoods separately, and provide Local Intrinsic Dimension (LID) estimation for each point in the dataset. Some of the typical algorithms are Manifold-Adaptive Dimension Estimation (MADE) [16], Maximum Likelihood Estimation (MLE) [34], and Geometry-aware MLE [21]. Both global and local IDs can be repurposed: global ID can be estimated by combining local ID estimations, while local ID can be estimated by applying global ID estimation within a local neighborhood. In the proposed AE-IDC framework, the ID estimator used is a global class estimator.

### C. The Effect of Intrinsic Dimension on DNNs

The change of ID is related to the change of geometrical properties of DNNs such as distribution, distance and curvature [35], [1], so ID is a quantitative characterization for understanding learning behavior from geometrical perspective. [29] constructed an ID-based framework to understand how compact representations are developed across layers in simplified neural networks. The work in [37], [33], [5] analyzed the effect of the ID on the generalization of DNNs. Ansuini *et al.* [1] found that the ID profile in trained DNNs follows a

hunchback shape, i.e. the ID first increases and then decreases, and the ID of the last hidden layer is crucial to the classifier’s performance. [36] found the shift of ID is an indication of the start of overfit in the learning process of DNNs on the dataset with noisy labels. [30] characterized the smoothness of data manifold by the knowledge of data representation’s ID.

Besides the effect on the generalization of DNNs, ID have effect on the robustness of DNNs. [1] attributes the rise of the ID profile to the redundant features, which are irrelevant to final task predictions. [39] revealed that high dimensional datasets are more difficult for DNNs to learn, and the dataset with higher ID value is more vulnerable to be adversarial perturbations. Moreover, the class with higher ID value is more vulnerable to attacks compared to other classes in the same image dataset. [35] found that adversarial attacks can raise the local ID value and train a local ID-based detector to remove adversarial examples from inputs of a classifier. However, to the best of our knowledge, there are few studies on explicitly controlling GID and LID of data representations to build a self-supervised representation models.

### III. THE PROPOSED SELF-SUPERVISED REPRESENTATION LEARNING FRAMEWORK WITH INTRINSIC DIMENSION REGULARIZATIONS

a) *Notation.*: Let  $\mathbf{X} \in \mathbb{R}^{N \times C \times H \times W}$  be a batch of inputs, where  $N, C, H, W$  are batch size, channel number, height and width respectively.  $\hat{\mathbf{X}}$  be the reconstruction of  $\mathbf{X}$ , and  $m$  is the number of total features.  $\tilde{\mathbf{X}} \in \mathbb{R}^{N \times m}$  is reshaped from  $\mathbf{X}$ , where  $m = C \times H \times W$ , and each feature of  $\tilde{\mathbf{X}}$  has been centralized for zero-mean. The covariance matrix of  $\mathbf{X}$  is denoted by  $\mathbf{C} = \tilde{\mathbf{X}}^\top \tilde{\mathbf{X}}$ . The data representation after a linear transformation is denoted as  $\mathbf{Y} = \tilde{\mathbf{X}}\mathbf{W}^\top \in \mathbb{R}^{N \times n}$ , where  $\mathbf{W}^\top \in \mathbb{R}^{m \times n}$  is the transformation matrix.

The synaptic and neural correlation were shown to be capable of controlling the dimensionality of hidden representations in DNNs [29], [44]. Based on this phenomenon, Huang [29] defines an ID estimator for the hidden representation at each layer,

$$\mathbf{ID}(\mathbf{X}) = \frac{(\text{tr}(\mathbf{C}))^2}{\text{tr}(\mathbf{C}^2)} = \frac{(\sum_i e_i)^2}{\sum_i e_i^2}, \quad (1)$$

where  $\mathbf{C}$  is the covariance matrix of data representations, and  $e_i$  is the eigenvalue of  $\mathbf{C}$ . This estimator considers pairwise correlations among synapses, and reveals the mechanism underlying how the synaptic and neural correlations affect dimension reduction [44]. Inspired by its success in characterizing the synaptic and neural correlation in physics and machine learning, in this work, we leverage Eq. (1) to estimate the global and local ID of data representations. We develop a novel self-supervised training framework to compress the original representations into a discriminative low dimensional space for downstream tasks, which reduces the variation of the global and local ID of representations along with pixel level reconstruction.

#### A. Control the Global and Local Intrinsic Dimensions of Data Representations.

Our framework builds upon a reconstruction-based AE, Stacked AutoEncoders (SAE), which is composed of multiple

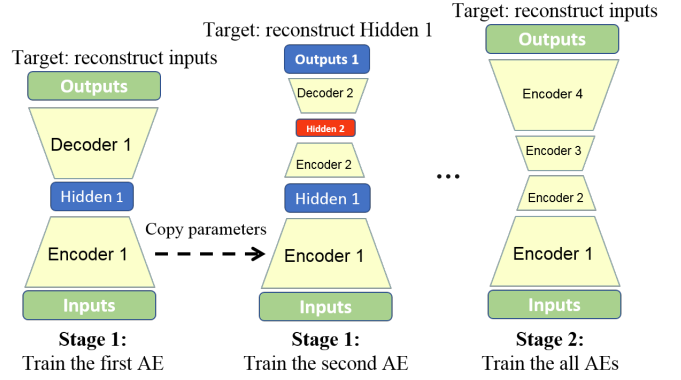


Fig. 2: Illustration of Two-stage training for AE-IDC. In this paper, a symmetric AE is used. The first half AEs are undercomplete, whose hidden representations are smaller than inputs; while the second half AEs are overcomplete, whose hidden representations are smaller than inputs.

AEs and has hierarchical architecture. The output of the previous AE is used as the input for the next AE. The training is two-stage: train single AE in layerwise manner first and then train the all AEs globally. Apart from SAE, the framework is also applicable to other AE variants.

The reconstruction loss of AE can be the Mean Squared Error (MSE) between the reconstructed and original images,

$$L(\mathbf{X}, \hat{\mathbf{X}}) = \frac{1}{N} \sum_{i=1}^N (\hat{x}_i - x_i)^2,$$

or the binary cross entropy loss,

$$L(\mathbf{X}, \hat{\mathbf{X}}) = -\frac{1}{N} \sum_{i=1}^N [x_i \log(\hat{x}_i) + (1 - x_i) \log(1 - \hat{x}_i)],$$

where  $x_i \in \mathbb{R}^{C \times H \times W}$  is a sample in  $\mathbf{X}$ . By minimizing the reconstruction loss, SAE learns a low-dimensional representations. However, this approach lacks the consideration about the variation of ID after reconstruction.

To address this issue, this paper proposes an effective framework named AutoEncoder with Intrinsic Dimension Constraint (AE-IDC), which introduce two extra constraints (GID and LID) to regularize the learning of AE.

The GID describes the geometric structure of the subspaces of varying dimensions from points in the batch. To compute the GID, the original inputs (batch, channel, height, weight) are reshaped into (batch, channel×height×weight). The GID is given by

$$\mathbf{GID}(\mathbf{X}) = \frac{(\text{tr}(\tilde{\mathbf{X}}^\top \tilde{\mathbf{X}}))^2}{\text{tr}((\tilde{\mathbf{X}}^\top \tilde{\mathbf{X}})^2)}, \quad (2)$$

Convolution kernels works as feature extractor and transform an input into multiple similar feature maps. We suppose that feature maps of the input indicates the local geometry of it. Considering that feature maps from the same data point are highly correlated, the space of these feature maps can be used as the description of the local geometric structure for the

point. We regard the ID of such space as the LID of the point. To compute the LID, the original sample (channel, height, weight) is reshaped into (channel, height $\times$ weight) first. The LID is then given by

$$\text{LID}(x_i) = \frac{(\text{tr}(\mathbf{M}^\top \mathbf{M}))^2}{\text{tr}((\mathbf{M}^\top \mathbf{M})^2)}, \text{ where } \mathbf{M} \in \mathbb{R}^{C \times HW}. \quad (3)$$

It is intuitive and reasonable that the variation of GID and LID between the original inputs and reconstruction needs to be as small as possible. Motivated by this consideration, we incorporate these two ID constraints into the reconstruction loss function to encourage the SAE to maintain ID. Formally, the objective optimized by a AE-IDC is

$$\begin{aligned} \mathcal{J}_{\text{AE-IDC}} = & L(\mathbf{X}, \hat{\mathbf{X}}) + \lambda_1 (\text{GID}(\mathbf{X}) - \text{GID}(\hat{\mathbf{X}}))^2 \\ & + \lambda_2 \sum_{i=1}^N (\text{LID}(x_i) - \text{LID}(\hat{x}_i))^2, \end{aligned} \quad (4)$$

where  $\lambda_1$  and  $\lambda_2$  are hyper-parameters controlling the strength of the corresponding regularization. Fig. 6 depict the performances of AE-IDC with respect to different weighing factors  $\lambda_1$  and  $\lambda_2$  in the downstream classification task.

Given most loss functions of the DNN models are mainly optimized by the backpropagation [22] for a batch of samples from the dataset, the differentiable geometrical structure characterization within the batch is needed. The reconstruction loss has been proven to be differentiable. The differential of IDC with respect to weight  $W$  of networks is computed as

$$\begin{aligned} \frac{\partial}{\partial \mathbf{W}} \left( \frac{\text{tr}(\mathbf{W}\mathbf{X}^\top \mathbf{X}\mathbf{W}^\top)^2}{\text{tr}(\mathbf{W}\mathbf{X}^\top \mathbf{X}\mathbf{W}^\top \mathbf{W}\mathbf{X}^\top \mathbf{X}\mathbf{W}^\top)} \right) = \\ (4t_2) / t_4 \cdot T_0 - (4t_2^2) / t_4^2 \cdot T_3, \end{aligned} \quad (5)$$

where

$$\begin{aligned} T_0 &= \mathbf{W}\mathbf{X}^\top \mathbf{X} \\ T_1 &= T_0 \mathbf{W}^\top \\ t_2 &= \text{tr}(T_1) \\ T_3 &= (T_1 \mathbf{W}\mathbf{X}^\top \mathbf{X}) \\ t_4 &= \text{tr}(T_3 \mathbf{W}^\top). \end{aligned}$$

Therefore, Eq. (4) is differentiable and can be incorporated into the back propagation.

### B. Two-stage Training of Autoencoder with Intrinsic Dimension Constraints

In the framework, we use an L-layer symmetric SAE, where the first  $L/2$  layers perform encoding and the second  $L/2$  layers perform decoding, shown in Fig. 2. Note that each layer is a separate AE, consisting of encoder and decoder parts. The first half AEs are undercomplete, and the second half AEs are overcomplete.

The training framework of AE-IDC is summarized in Algorithm 1. The framework also follows a two-stage paradigm. In the first stage, train the group of AEs in layerwise manner. During training the  $i^{\text{th}}$  AE, compute the reconstruction, and GID and LID loss according to this AE's input and output, then update the parameters of  $\text{AE}_i$  locally. In the second stage, stack all the pretrained AEs' encoder and perform end-to-end

### Algorithm 1: Training of AE-IDC.

---

**Input:**  $\mathcal{X}$ : a dataset of clean examples.  
 $\{\text{AE}_j\}_{j=1}^L$ :  $L$  AEs.  
 $f_{enc}^i$ : the encoder of  $\text{AE}_i$ ;  $f_{dec}^i$ : the decoder of  $\text{AE}_i$ .  
**Output:** The encoder part of the SAE.

- 1 # Layerwise training for each AE.
- 2 **for**  $i = 1$  **to**  $l$  **do**
- 3     Freeze all the previous AEs  $\{\text{AE}_j\}_{j=1}^{i-1}$ .
- 4     **for** *sample a batch*  $\mathbf{X}$  *from*  $\mathcal{X}$  **do**
- 5         input of  $\text{AE}_i$ :  $\mathbf{X}_i = f_{enc}^{i-1}(\mathbf{X}_{i-1})$ , where  $\mathbf{X}_1 = \mathbf{X}$ .
- 6         compute *loss* according to Eq. (4).
- 7         perform BP to update parameters of  $\text{AE}_i$  by minimizing *loss*.
- 8 # Global training for whole AEs.
- 9 Stack all the encoders  $\{f_{enc}^i\}_{i=1}^L$  to construct a SAE.
- 10 **for** *sample a batch*  $\mathbf{X}$  *from*  $\mathcal{X}$  **do**
- 11     compute *loss* according to Eq. (4).
- 12     perform BP to update parameters of SAE by minimizing *loss*.

---

Dataset	Training Set	Testing Set	Class
Extended Yale B [19]	2314	1874	38
Caltech101 [17]	6907	1770	101
ImageNet10 [41]	13000	478	10
ImageNet-1K [41]	1281167	50000	1000

TABLE I: Configuration of Datasets

training to update the parameters of  $\{f_{enc}^i\}_{i=1}^L$  globally. At inference, we only take the first half of the trained AE-IDC to perform feature extraction for downstream tasks.

## IV. EXPERIMENTS

To validate the proposed AE-IDC, we first investigate the effect of IDC imposed on the training of models. Then, evaluate the feature extracting performance of the proposed AE-IDC on two downstream tasks: image classification and clustering. Finally, conduct extensive ablation studies to analyze the impact of different components of AE-IDC.

a) *Datasets.*: In this section, the performance of the proposed method AE-IDC is validated by experiments on three benchmark image datasets including Extended Yale B, Caltech101, and ImageNet. ImageNet10 is a subset of ImageNet-1K, which consists of ten classes selected from ImageNet-1K. It provides a fast test tool on on ImageNet without loss of generality. The configurations about the splitting of datasets in this work are summarized in Tab. I.

b) *Implementation Settings.*: We mainly use convolution, deconvolution, maxpooling and upsampling layers to construct SAE. The details about architectures of AE used in the following subsections can refer to appendix. For large-scale dataset, we adopt the standard ViT-Base (ViT-B) [14]. Weights of regularizers are set  $\lambda_1 = 0.1$  and  $\lambda_2 = 0.1$  as default. All experiments in this paper are conducted on an NVIDIA RTX

3090 GPU (2 GB memory). And the codes for the reproduction of our work will be available at Github.

### A. Analysis of AE-IDC’s Learning Process

a) *CNNs-based AE-IDC.*: To simplify the analysis, we analyze the CNNs model used in Extended Yale B, which only consists of four convolutional layers, where the extrinsic dimension of data representations is (3,32,32)-(12,16,16)-(24,8,8)-(12,16,16)-(3,32,32) from inputs to reconstructions. The figure depicting the full loss landscapes of two SAE models with and without IDC during two-stage training is attached in appendix. The reconstruction loss of both models gradually converges at the end of 100 epochs’ training in the layerwise and global training stages. But SAE-IDC’s reconstruction loss is a bit higher than vanilla SAE. This is because the SAE-IDC is regularized to learn a more abstract embedding feature space instead of a simple reconstruction of pixels. For global and local ID loss, SAE-IDC achieves smoother training curves and quicker convergences in the layerwise and global training stages, compared to vanilla SAE. It can obviously observed that for LID loss vanilla SAE do not converge at the first step layerwise training and the final global training. We suppose that the convergence of reconstruction, global and local ID loss is the reason for SAE-IDC to extract discriminative representations for downstream tasks.

b) *ViT-based AE-IDC.*: MAE [25], a form of DAE, is a State-Of-The-Art (SOTA) self-supervised learner in AE-based learners. However, MAE only utilizes MSE as its reconstruction target, which ignore the geometric structure information. We will show in following subsection that the enhanced MAE under the proposed IDC, dubbed as MAE-IDC, will unleash the potential of MAE. Fig. 3 shows the landscape of three kinds of loss. We use pretrained model from [25] to initialize all models. The MAE without ID constraint has reached its optimal point at the start, resulting in its losses remaining nearly constant. Conversely, the MAE variants with ID constraints converge quickly after ten epochs, with the GID loss and LID loss dropping after imposing the corresponding regularizer. All these MAE variants keep the reconstruction ability, shown in Fig. 4.

### B. Evaluation of Representations on Downstream Tasks

We choose image classification and clustering as downstream tasks. The performance of embedded representations is evaluated on the classification task using K-Nearest Neighbor (KNN) algorithm, and on the clustering task using K-means algorithm. The KNN and K-means algorithms provide a fast test, without the need to carry on a heavy end-to-end fine-tuning, and also provide relative fairness for comparison. The number of time to run k-means is ten.

a) *Results on Classification Tasks.*: To demonstrate the generality of the proposed algorithmic framework, we apply this framework into two other widely used AE variants, i.e., DAE and sparse AE. As seen in Tab. II, for CNNs-based models, AE-IDC outperforms AE without IDC on all three datasets by 1% ~ 5%. We also compare AE-IDC with SOTA self-supervised learning methods on ImageNet10 and ImageNet-1K. For fair comparison, let the compared methods use its

Method	Arch.	Dim.	k=5	k=10	k=15
Extended Yale B					
SAE	CNNs	(24,8,8)	82.28	81.75	79.19
SAE-IDC	CNNs	(24,8,8)	<b>86.50</b>	<b>83.78</b>	<b>81.96</b>
DAE	CNNs	(24,8,8)	66.70	62.75	59.34
DAE-IDC	CNNs	(24,8,8)	<b>69.65</b>	<b>65.47</b>	<b>62.65</b>
SparseAE	CNNs	(24,8,8)	82.07	81.22	81.22
SparseAE-IDC	CNNs	(24,8,8)	<b>84.85</b>	<b>84.63</b>	<b>83.30</b>
Caltech101					
SAE	CNNs	(24,28,28)	49.49	43.39	39.66
SAE-IDC	CNNs	(24,28,28)	<b>50.33</b>	<b>45.48</b>	<b>42.20</b>
ImageNet10					
SAE	CNNs	(512,7,7)	34.94	33.47	33.26
SAE-IDC	CNNs	(512,7,7)	<b>35.77</b>	<b>36.19</b>	<b>35.56</b>
MAE[25]	ViT-B	768	74.89	75.52	75.94
MAE-IDC	ViT-B	768	<b>75.94</b>	<b>76.56</b>	<b>76.98</b>
MoCo v3 [11]	ViT-B	768	27.61	28.03	29.91
DINO [7]	ViT-B	768	73.22	73.64	76.35
ImageNet-1K					
MAE[25]	ViT-B	768	49.03	45.82	43.94
MAE-IDC	ViT-B	768	49.14	45.93	44.06
MoCo v3 [11]	ViT-B	768	27.61	28.03	29.91
DINO [7]	ViT-B	768	67.32	63.97	62.30

TABLE II: Classification performance (metric: Average Top-1 Accuracy(%)) on Extended Yale B, Caltech-101 and ImageNet datasets, where a KNN classifier is applied after feature extraction.

public official fine-tuned models without any modification. as shown in Table II. Though MAE-IDC only wins the best performance by 0.1% on ImageNet-1K, its training process is more concise and easy to understand.

b) *Results on Clustering Tasks.*: The metrics for evaluation are Adjusted Mutual Index (AMI) and Adjusted Rand Index (ARI). All models are pretrained on ImageNet-1K. The results in Tab. III shows MAE-IDC’s advantage over MAE on clustering task. This is in coordinated with visualization results in Fig. 5. Although MAE-IDC falls behind the SOTA contrastive learning DINO, the gap shrinks on Caltech101.

Method	ImageNet10	Caltech101
MAE[25]	0.280  0.451	0.293  0.532
MAE-IDC	<b>0.291  0.467</b>	<b>0.313  0.542</b>
MoCo v3 [11]	0.090  0.189	0.047  0.112
DINO [7]	0.491  0.645	0.328  0.576

TABLE III: Clustering performance (metric: ARI||AMI) of the proposed AE-IDC with comparisons to three SOTA self-supervised methods, where K-means algorithm applied after feature extraction. The configuration of architecture and embedding dimension is same with Tab. II.

### C. Ablation studies

In this subsection, we ablate the design of AE-IDC, and analyze the impacts of elements in loss function, stagewise training and weights of regularizers for the performance of AE-IDC.

a) *Elements in Loss Function.*: We demonstrate the classification accuracy of models trained with three variants

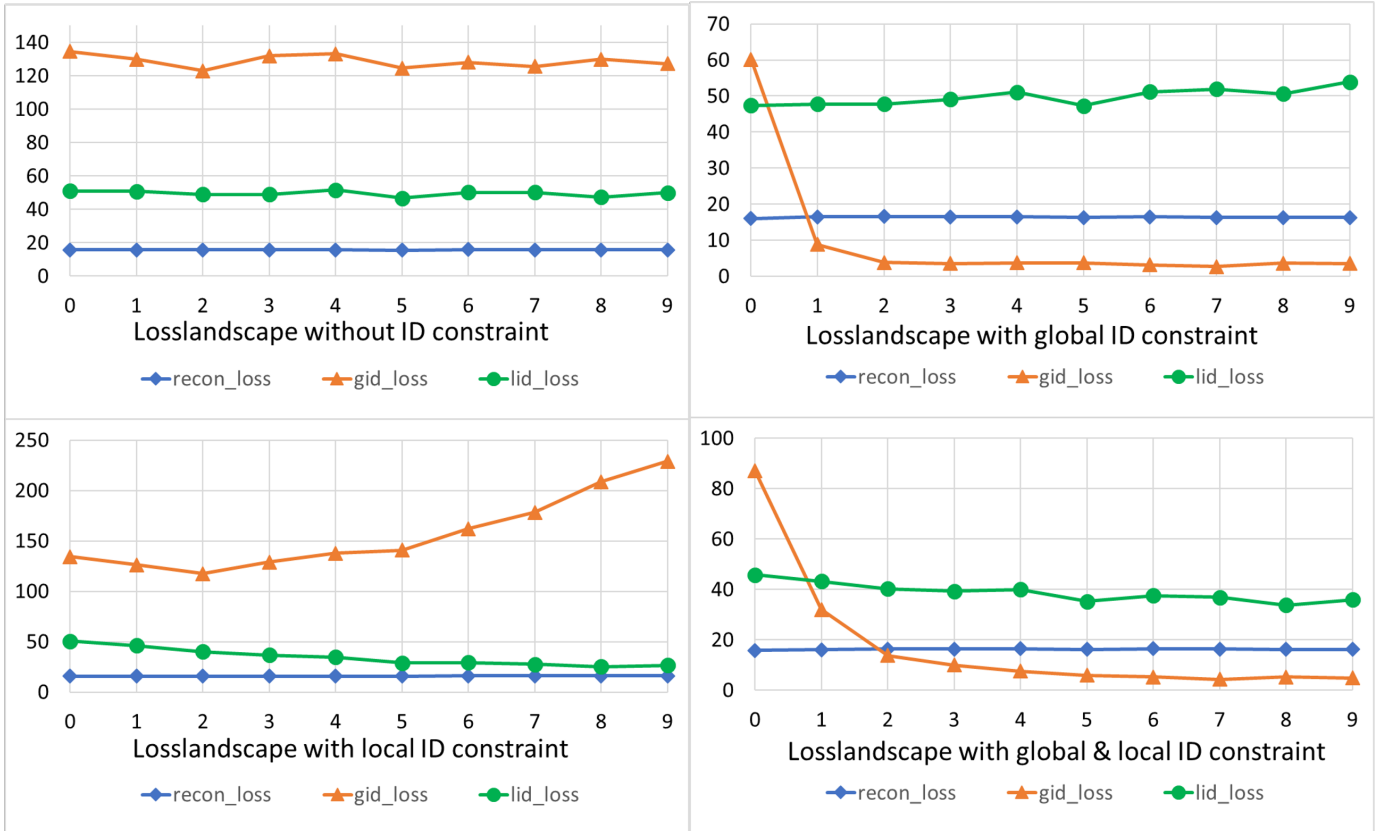


Fig. 3: Loss landscapes of MAE and its variants with different intrinsic dimension constraints on ImageNet10. The horizontal axis represents the number of epochs, and the vertical axis represents the loss value. All these four MAEs are initialized with the same pretrained model.

Loss Item	KNN Accuracy
Reconstruction (Baseline)	82.28
Reconstruction + GID	83.99
Reconstruction + LID	83.78
Reconstruction + GID + LID	<b>86.50</b>
GID + LID	59.98

TABLE IV: Impact of the each component in the proposed loss function (Eq. (4)) to the KNN recognition rate on the Extended Yale B.

of loss Function: **Reconstruction+GID, Reconstruction+LID** and **GID+LID**. As shown in Tab. IV, the reconstruction loss is the most significant factor influencing the quality of the learned representations. While using GID and LID loss separately is insufficient for the learning of AE-IDC. Therefore, ID constraints should be combined with the reconstruction loss, and there exists a synergistic relationship between the GID regularizer and LID regularizer.

*b) Stagewise Training.*: Here we compare the two-stage training with two training variants: one-stage layerwise training and one-stage global learning. Tab. V demonstrate the efficacy of the two-stage training, which is superior than both one-stage layerwise training and one-stage global learning. The results in Tab. V also validate that one-stage layerwise training or global training can learn more effective representa-

Training Paradigm	KNN Accuracy
Baseline	82.28
Layerwise training	83.88
Global training	85.92
Layerwise training + Global training	<b>86.50</b>

TABLE V: Impact of each stage in the proposed two-stage training paradigm of AE-IDC in Algorithm 1 to the KNN recognition rate on the Extended Yale B.

tions, compared to the baseline. There in the resource-limited situations, using one-stage global training can be an option to reduce the training time.

*c) Weight of Regularizers.*: We investigate the impact of two critical hyper-parameters  $\lambda_1$  and  $\lambda_2$ : the weights for the GID regularizer and LID regularizer respectively. Fig. 6 demonstrate that IDC is not highly sensitive to the choice of these weights. This alleviates the need for extensive fine-tuning and facilitates the implementation of our approach on the customized dataset.

## V. CONCLUSIONS

In this work, we proposed a novel regularized autoencoder for representation learning, which exploits data representations' global and local ID information, coined as AE-IDC. Specifically, we regard the ID of the manifold formed by the

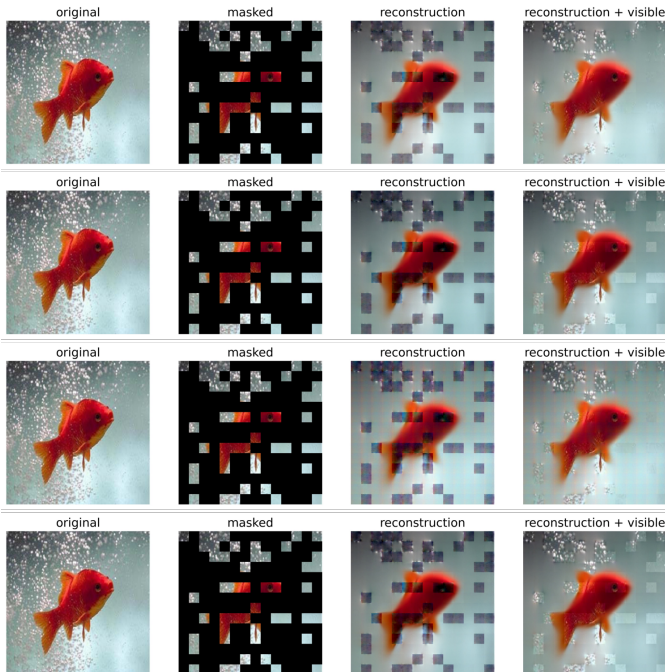


Fig. 4: Reconstructions of a 75% masked image from ImageNet through MAE, MAE with GID regularizer, MAE with a LID regularizer and MAE-IDC, from top to bottom.

same batch of images as the estimation of the global ID of this batch of images, and the ID of the manifold formed by matrices of different channels in the same image as the local ID estimate of the image. We suppose that global and local ID should remain invariant as much as possible between the reconstruction by the regularized autoencoder and original inputs. Our empirical results validate the efficient representation achieved by the encoder of AE-IDC on different downstream tasks. Our work is limited to the area of DNNs, but it will motivate the future development of other representation-learning algorithms like the probabilistic models and the manifold-learning approaches to exploit the information about the topological structure of the representations' dimensions.

## REFERENCES

- [1] Alessio Ansuini, Alessandro Laio, Jakob H. Macke, and Davide Zoccolan. Intrinsic dimension of data representations in deep neural networks. In *NeurIPS*, pages 6109–6119, 2019. 1, 2, 3
- [2] Jonathan Bac, Evgeny M Mirkes, Alexander N Gorban, Ivan Tyukin, and Andrei Zinovyev. Scikit-dimension: a python package for intrinsic dimension estimation. *Entropy*, 23(10):1368, 2021. 1, 2
- [3] Hangbo Bao, Li Dong, and Furu Wei. Beit: Bert pre-training of image transformers. In *ICLR*, 2022. 1
- [4] Yoshua Bengio, Aaron Courville, and Pascal Vincent. Representation learning: A review and new perspectives. *PAMI*, 35(8):1798–1828, 2013. 1
- [5] Tolga Birdal, Aaron Lou, Leonidas J. Guibas, and Umut Simsekli. Intrinsic dimension, persistent homology and generalization in neural networks. In Marc’Aurelio Ranzato, Alina Beygelzimer, Yann N. Dauphin, Percy Liang, and Jennifer Wortman Vaughan, editors, *NeurIPS*, pages 6776–6789, 2021. 2
- [6] Pratik Prabhajan Brahman, Dapeng Wu, and Yiyuan She. Why deep learning works: A manifold disentanglement perspective. *TNNLS*, 27(10):1997–2008, 2015. 1
- [7] Mathilde Caron, Hugo Touvron, Ishan Misra, Hervé Jégou, Julien Mairal, Piotr Bojanowski, and Armand Joulin. Emerging properties in self-supervised vision transformers. In *ICCV*, 2021. 2, 5

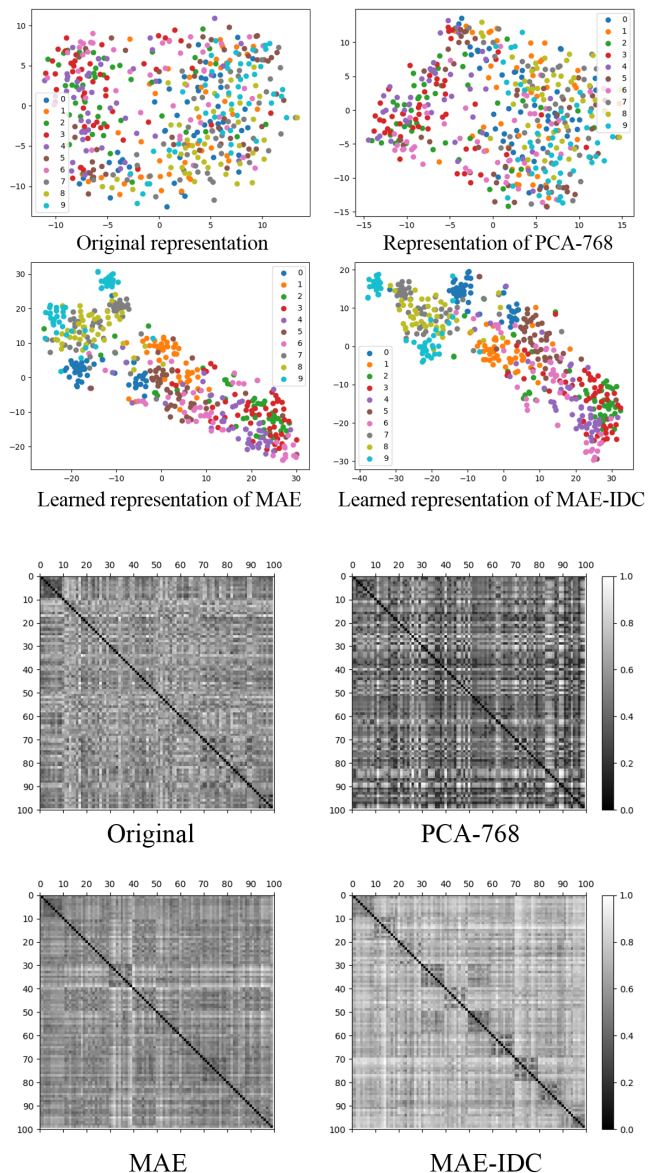


Fig. 5: Visualization of self-supervisedly learned representations on the test set of ImageNet10 using t-SNE (Top group), and geodesic distance distributions between ten classes from ImageNet10 with each class has ten images (Bottom group). The geodesic distance is computed approximately by KNN graph euclidean distance where  $K=15$ , and is linearly rescaled to  $[0, 1]$  for the convenient of visualization. The distribution of geodesic distance is decentralized in the original space and the linear subspace by PCA. Compared to MAE, MAE-IDC is more centralized in diagonal, which means it keeps the manifold structure, i.e., the similarity in the same class and dissimilarity between different classes.

- [8] Claudio Ceruti, Simone Bassis, Alessandro Rozza, Gabriele Lombardi, Elena Casiraghi, and Paola Campadelli. Danco: An intrinsic dimensionality estimator exploiting angle and norm concentration. *Pattern recognition*, 47(8):2569–2581, 2014. 2
- [9] Liang-Chieh Chen, George Papandreou, Iasonas Kokkinos, Kevin Murphy, and Alan L Yuille. Deeplab: Semantic image segmentation with deep convolutional nets, atrous convolution, and fully connected crfs.

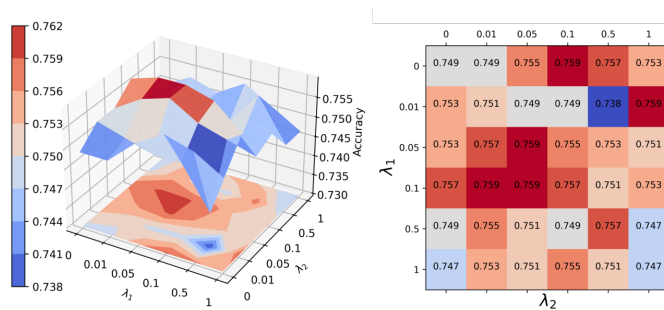


Fig. 6: Impact of the weights of regularizers to the recognition rate of KNN on ImageNet10. The 3D contour plot is generated from the discrete heatmaps displayed on the right-hand side.

- PAMI*, 40(4):834–848, 2018. 1
- [10] Ting Chen, Simon Kornblith, Mohammad Norouzi, and Geoffrey Hinton. A simple framework for contrastive learning of visual representations. In *ICML*, pages 1597–1607, 2020. 2
- [11] Xinlei Chen, Saining Xie, and Kaiming He. An empirical study of training self-supervised vision transformers. In *ICCV*, pages 9620–9629, 2021. 5
- [12] Francois Chollet. Xception: Deep learning with depthwise separable convolutions. In *CVPR*, pages 1800–1807, 2017. 1
- [13] Carl Doersch, Abhinav Gupta, and Alexei A Efros. Unsupervised visual representation learning by context prediction. In *ICCV*, pages 1422–1430, 2015. 1
- [14] Alexey Dosovitskiy, Lucas Beyer, Alexander Kolesnikov, Dirk Weissenborn, Xiaohua Zhai, Thomas Unterthiner, Mostafa Dehghani, Matthias Minderer, Georg Heigold, Sylvain Gelly, Jakob Uszkoreit, and Neil Houlsby. An image is worth 16x16 words: Transformers for image recognition at scale. In *ICLR*, 2021. 2, 4
- [15] Elena Facco, Maria d’Errico, Alex Rodriguez, and Alessandro Laio. Estimating the intrinsic dimension of datasets by a minimal neighborhood information. *Scientific Reports*, 7:12140, 2017. 1, 2
- [16] Amir Massoud Farahmand, Csaba Szepesvári, and Jean-Yves Audibert. Manifold-adaptive dimension estimation. In *ICML*, pages 265–272, 2007. 2
- [17] Li Fei-Fei, Rob Fergus, and Pietro Perona. Learning generative visual models from few training examples: An incremental bayesian approach tested on 101 object categories. In *CVPRW*, pages 178–178, 2004. 2, 4
- [18] Peng Gao, Teli Ma, Hongsheng Li, Ziyi Lin, Jifeng Dai, and Yu Qiao. MCMAE: Masked convolution meets masked autoencoders. In *NeurIPS*, 2022. 2
- [19] Athinodoros S. Georghiades, Peter N. Belhumeur, and David J. Kriegman. From few to many: Illumination cone models for face recognition under variable lighting and pose. *PAMI*, 23(6):643–660, 2001. 2, 4
- [20] Spyros Gidaris, Praveer Singh, and Nikos Komodakis. Unsupervised representation learning by predicting image rotations. In *ICLR*, 2018. 1
- [21] Marina Gomtsyan, Nikita Mokrov, Maxim Panov, and Yury Yanovich. Geometry-aware maximum likelihood estimation of intrinsic dimension. In *ACML*, 2019. 2
- [22] Ian Goodfellow, Yoshua Bengio, and Aaron Courville. *Deep Learning*. MIT Press, 2016. <http://www.deeplearningbook.org>. 2, 4
- [23] Ian J. Goodfellow, Jean Pouget-Abadie, Mehdi Mirza, Bing Xu, David Warde-Farley, Sherjil Ozair, Aaron C. Courville, and Yoshua Bengio. Generative adversarial nets. In Zoubin Ghahramani, Max Welling, Corinna Cortes, Neil D. Lawrence, and Kilian Q. Weinberger, editors, *NeurIPS*, pages 2672–2680, 2014. 2
- [24] Peter Grassberger and Itamar Procaccia. Measuring the strangeness of strange attractors. *Physica D: Nonlinear Phenomena*, 9:189–208, 1983. 2
- [25] Kaiming He, Xinlei Chen, Saining Xie, Yanghao Li, Piotr Dollár, and Ross B. Girshick. Masked autoencoders are scalable vision learners. In *CVPR*, pages 15979–15988, 2022. 1, 2, 5
- [26] Kaiming He, Haoqi Fan, Yuxin Wu, Saining Xie, and Ross Girshick. Momentum contrast for unsupervised visual representation learning. In *CVPR*, pages 9729–9738, 2020. 2
- [27] Kaiming He, Xiangyu Zhang, Shaoqing Ren, and Jian Sun. Identity mappings in deep residual networks. In *ECCV*, volume 9908, pages 630–645, 2016. 2
- [28] Zhen He, Shaobing Gao, Liang Xiao, Daxue Liu, Hangen He, and David Barber. Wider and deeper, cheaper and faster: Tensorized lstms for sequence learning. In *NeurIPS*, pages 1–11, 2017. 1
- [29] Haiping Huang. Mechanisms of dimensionality reduction and decorrelation in deep neural networks. *Physical Review E*, 98(6):062313, 2018. 2, 3
- [30] Zijian Jiang, Jianwen Zhou, and Haiping Huang. Relationship between manifold smoothness and adversarial vulnerability in deep learning with local errors. *Chinese Physics B*, 30(4):048702, 2021. 3
- [31] Longlong Jing and Yingli Tian. Self-supervised visual feature learning with deep neural networks: A survey. *PAMI*, 43(11):4037–4058, 2020. 1
- [32] Diederik P Kingma and Max Welling. Auto-encoding variational bayes. In *ICLR*, 2014. 2
- [33] Fabian Latorre, Leello Tadesse Dadi, Paul Rolland, and Volkan Cevher. The effect of the intrinsic dimension on the generalization of quadratic classifiers. In *NeurIPS*, volume 34, pages 21138–21149, 2021. 2
- [34] Elizaveta Levina and Peter J. Bickel. Maximum likelihood estimation of intrinsic dimension. In *NeurIPS*, pages 777–784, 2004. 1, 2
- [35] Xingjun Ma, Bo Li, Yisen Wang, Sarah M. Erfani, Sudanthi N. R. Wijewickrema, Grant Schoenebeck, Dawn Song, Michael E. Houle, and James Bailey. Characterizing adversarial subspaces using local intrinsic dimensionality. In *ICLR*, 2018. 2, 3
- [36] Xingjun Ma, Yisen Wang, Michael E. Houle, Shuo Zhou, Sarah M. Erfani, Shu-Tao Xia, Sudanthi N. R. Wijewickrema, and James Bailey. Dimensionality-driven learning with noisy labels. In Jennifer G. Dy and Andreas Krause, editors, *ICML*, volume 80, pages 3361–3370, 2018. 3
- [37] Ryumei Nakada and Masaaki Imaizumi. Adaptive approximation and generalization of deep neural network with intrinsic dimensionality. *J. Mach. Learn. Res.*, 21:174–1, 2020. 2
- [38] Deepak Pathak, Philipp Krahenbuhl, Jeff Donahue, Trevor Darrell, and Alexei A. Efros. Context encoders: Feature learning by inpainting. In *CVPR*, June 2016. 1
- [39] Phillip Pope, Chen Zhu, Ahmed Abdelkader, Micah Goldblum, and Tom Goldstein. The intrinsic dimension of images and its impact on learning. In *ICLR*, 2021. 3
- [40] Sam T Roweis and Lawrence K Saul. Nonlinear dimensionality reduction by locally linear embedding. *Science*, 290(5500):2323–2326, 2000. 1
- [41] Olga Russakovsky, Jia Deng, Hao Su, Jonathan Krause, Sanjeev Satheesh, Sean Ma, Zhiheng Huang, Andrej Karpathy, Aditya Khosla, Michael Bernstein, et al. Imagenet large scale visual recognition challenge. *IJCV*, 115(3):211–252, 2015. 2, 4
- [42] Joshua B Tenenbaum, Vin De Silva, and John C Langford. A global geometric framework for nonlinear dimensionality reduction. *Science*, 290(5500):2319–2323, 2000. 1
- [43] Pascal Vincent, Hugo Larochelle, Yoshua Bengio, and Pierre-Antoine Manzagol. Extracting and composing robust features with denoising autoencoders. In *ICML*, page 1096–1103, 2008. 2
- [44] Jianwen Zhou and Haiping Huang. Weakly correlated synapses promote dimension reduction in deep neural networks. *Physical Review E*, 103(1):012315, 2021. 3
- [45] Peicheng Zhou, Junwei Han, Gong Cheng, and Baochang Zhang. Learning compact and discriminative stacked autoencoder for hyperspectral image classification. *IEEE Transactions on Geoscience and Remote Sensing*, 57(7):4823–4833, 2019. 1